Metabolomics Analysis Reveals Interaction of Base-Line Chemotherapy and Shiyiwei Shenqi Tablets in Breast Cancer Treatment

Hong Wan[1†], Xiaojun Xu[2,3†], Xiaowei Yang[2,3†], Angqing Li[3], Xiaopeng Ma[4], Aman Xu[1], Xiao Yuan[1], Wenbin Wang[1], Tao Guo[1], Guangtao Luo[2,3], Xiaobo He[3], Wang Li[5], Zhaorui Wang[2,3], Qiang Sun[6], Jing Pei[2,3]*, Yongzhen Guo[7]* and Yong Zhu[1]*

[1]Department of General Surgery, The Fourth Affiliated Hospital of Anhui Medical University, Hefei, China, [2]Department of Breast Surgery, The First Affiliated Hospital of Anhui Medical University, Hefei, China, [3]Department of General Surgery, The First Affiliated Hospital of Anhui Medical University, Hefei, China, [4]Department of Thyroid and Breast Surgery, The First Affiliated Hospital of University of Science and Technology of China, Hefei, China, [5]Department of Head and Neck Surgery, The First Affiliated Hospital of University of Science and Technology of China, Hefei, China, [6]Cancer Institute, Xuzhou Medical University, Xuzhou, China, [7]Department of Pathology, The Third Affliated Hospital of Zhengzhou University, Zhengzhou, China

Shiyiwei Shenqi Tablet (SSTs) has been widely used for treatment of different types of cancer including breast cancer. SST has drawn more and more interest due to the low rate of side effects. The aim of this study was to investigate the metabolites in serums of breast cancer patients who received base-line chemotherapy only or combination treatment with SST. An untargeted metabolomics method was developed to investigate the alteration of metabolism in patients' serums using ultra-high-performance liquid chromatography/ Q-exactive Orbitrap mass spectrometry. The patients were separated based on the metabolomics data, and further analyses showed that SST treatment can affect the metabolism of glucose, fatty acid, bile acid and amino acid. In particular, SST treatment significantly reduced some short peptides which are potential tumor neoantigens. This study may provide novel insights into the mechanism underlying interaction between SST and base-line chemotherapy in terms of affecting metabolic pathways and thereby changing metabolic products, which might shed new light for clinical medication.

Keywords: shiyiwei shenqi tablets, breast cancer, untargeted metabolomics, amino acid metabolism, side effects

INTRODUCTION

Breast cancer is the leading female cancer (2,261,419 cases worldwide in 2020) and the leading cause of cancer-related deaths around the world (684,996 deaths worldwide in 2020) (DeSantis et al., 2019; Sung et al., 2021). Despite dramatic improvements achieved in breast cancer diagnosis and treatments, the prognosis of breast cancer patients, especially those with metastasis, remains unsatisfactory (Miller et al., 2019). In China, the breast cancer incidence and mortality are rising (Chen et al., 2016). According to the report of Centers for disease Control of China, breast cancer has become the most common cancer type in Chinese women. There were 416,371 new breast cancer cases in 2020 in China, and 117,174 breast cancer-induced death in 2020, which impose a heavy burden on the public health system (Cao et al., 2021). The influence of some recognized risk factors such as alcohol use, tobacco use, hormone levels, and body weight on breast cancer generation, and the roles of metabolism in breast cancer etiology and treatment remain unclear and need further study (Li et al., 2016).

Metabolomics is characterized as a technique that can comprehensively and simultaneously identify small molecule metabolites and quantify their changes under different conditions (Johnson et al., 2016; Cui et al., 2018; Jang et al., 2018; Guo et al., 2019). Metabolomics aims to identify indicators to reflect interactions between biological systems. So, it is an ideal holistic method for investigation of drug-drug interactions to obtain further insights into pharmacodynamic mechanisms (Kalwat and Cobb, 2017). Non-targeted metabolomics provides high-throughput analysis of metabolites in samples, which is very helpful for investigating new drug-drug interactions (Li et al., 2017; Zhang et al., 2020). Several analytical platforms including nuclear magnetic resonance (NMR), high performance liquid chromatography mass spectrometry (HPLC-MS), and gas chromatography mass spectrometry (GC-MS) are used for non-targeted metabolomics analysis (Alonso et al., 2015). MS based metabolomics approaches have been widely applied due to their high throughput and sensitivity, and highly quantitative and reproducible data (Cui et al., 2018). Furthermore, the negative and positive ionization also enhances the examination sensitivity.

Although surgery chemotherapy, radiotherapy, and targeted therapy have been combined and widely utilized for breast cancer treatment, recurrence and metastasis remain leading to a high mortality of advanced breast cancer patients (Harbeck et al., 2019). Furthermore, chemotherapy can lead to substantial side effects as well as drug resistance, resulting in therapeutic failure eventually (Ponde et al., 2019). Therefore, it is urgent to seek novel treatment methods for breast cancer. Traditional Chinese medicine (TCM) has been widely used to treat various types of cancers (Yan et al., 2017; Xiang et al., 2019), particularly, TCM has been applied in almost half patients who have breast cancer in China (Poo et al., 2020; Yang et al., 2021). Notably, the utilization of TCM in Western countries is also rising. Previous studies showed that the extract of *Astragalus* membranaceus can induce apoptosis of several breast cancer cells *via* suppressing PI3K/AKT/mTOR pathway (Zhou et al., 2018; Liu et al., 2019). Scutellaria barbata plus Hedyotis diffusa has shown high efficacy in breast cancer therapy (Fang et al., 2020). These studies indicate the promising prospects of TCM in breast cancer therapy.

TCM has drawn more and more interest due to its high safety and efficacy, low toxicity and side effects, as well as potential synergistic effects when combined with chemotherapy (Xiang et al., 2019). Shiyiwei Shenqi Tablet (SST) is a traditional Chinese decoction that has been utilized for treatment of leucopenia and relief of chemotherapy related symptoms: lassitude, vomiting, weakness, nausea, emaciation, and dizziness. SST consists of 11 Chinese herbs including Panax ginseng C. A. Mey, *Astragalus* abbreviatus Kar. and Kir, Angelica acutiloba (Siebold & Zucc.) Kitag, Gastrodia elata Blume, Rehmannia glutinosa (Gaertn.) DC, Catsia tora Linn, Rhizoma Alismatis, Cuscuta abyssinica A. Rich, Asarum acuminatum (Ashe), E. P. Bicknell, Cornu Cervi, and Lycium chinense Mill) (Dong et al., 2010; Chen et al., 2011; Yang et al., 2017). The mechanisms of pharmacodynamics and drug-drug interaction for SST still remain unclear. Moreover, the

influence of compounds on metabolism of each other is very complicated. Therefore, new strategy is needed to investigate the drug-drug interactions in combination treatment with base-line chemotherapy and SST. In this study, we performed non-targeted metabolomics analysis using HPLC-MS to explore the interactions between base-line chemotherapy and SST in breast cancer treatment. Patients with sole base-line chemotherapy treatment or combination treatments were prospectively enrolled, and the changes of metabolites in serum were examined to elucidate the mechanism of interaction between base-line chemotherapy and SST.

MATERIALS AND METHODS

Study Subjects
30 Chinese female patients aged from 30 to 70 years with a definite diagnosis of breast cancer were prospectively enrolled. The clinicopathological characteristics of the patients involved were assessed independently by two senior pathologists. In addition, patients with any prior treatment for breast cancer, preinvasive carcinoma, distant metastasis, other malignancies, active rheumatism, or heart failure were excluded. All the involved patients were informed about the participation benefits and risks, and were provided written informed consent. Studies were approved by the Institutional Review Board of the Fourth Affiliated Hospital of Anhui Medical University, and conducted in compliance with the Declaration of Helsinki principles (PJ-YX2020-011).

Study Design
The 30 patients were randomly divided into two groups: 1) base-line chemotherapy treatment group (n = 15); 2) adjuvant SST treatment group (n = 15). Patients from the adjuvant SST treatment group were given epirubicin combined with cyclophosphamide as the neoadjuvant chemotherapy and SST. Patients from the base-line chemotherapy treatment group received epirubicin combined with cyclophosphamide as neoadjuvant therapy. The dosages of epirubicin and cyclophosphamide were 90 mg/m^2 and 600 mg/m^2 per course, respectively. The dosage of SST was 2 g three times a day. Before treatment and 14 days after treatment, the whole blood samples were clot and centrifuged for 10 min at 1,000×g, and serum was isolated and stored at −80 ˚C until further use.

Formula of SST
First, Panax ginseng C.A.Mey [Araliaceae; Panax quinquefolius var. ginseng], 67 g *Astragalus* mongholicus Bunge [Fabaceae; Astragalus membranaceus Fisch. ex Bunge], 89 g Angelica sinensis (Oliv.) Diels [Apiaceae; Angelica polymorpha var. sinensis Oliv], 44.5 g Gastrodia elata Blume [Orchidaceae; Gastrodia elata var. gracilis Pamp], 89 g Rehmannia glutinosa (Gaertn.) DC. [Orobanchaceae; Rehmannia Libosch. ex Fisch. and C.A.Mey.], 66.5 g Alisma plantago-aquatica subsp. orientale (Sam.) Sam. [Alismataceae; Alisma plantago-aquatica var. orientale Sam.], 89 g *Senna* tora (L.) Roxb. [Fabaceae; *Cassia* contorta Vogel], 22 g Cornu Cervi Pantotrichum [Cervidae;

antler of *Cervus* nippon Temminck], 66.5 g Cuscuta chinensis Lam. [Convolvulaceae; Pentake chinense (Lam.) Raf.], 2.5 g Asarum sieboldii Miq. [Aristolochiaceae; Asarum sieboldii var. cornutum Y.N.Lee], 66.5 g Lycium barbarum L. [Solanaceae; Lycium barbarum Thunb.]. All of these herbs were grounded into powder. The powder were then boiled at high pressure for 20 h. Further, the residues were filtrated, and the paste was concentrated to a relative density of 1.20–1.25 (55–60°C) at reduced pressure, then spray-dried and crushed into fine powder. Finally, the sucrose were added to the powder to make 1000 g SST.

Untargeted Metabolomics Analysis

Sample preparation: The metabolites in serum were identified using HPLC-MS. For HPLC-MS analysis, 200 μL serum sample was added into a tube with 1,200 μL ice methanol and acetonitrile (50/50, v/v). After a 10-min standing at -20°C, the solution was centrifuged for 10 min at 10000 rpm. Then the supernatant was dried by rotary evaporation, and 50 μL acetonitrile was added for re-dissolving and further analysis by LC-MS.

LC-MS conditions: LC experiment was conducted on a waters e2695 UPLC (waters, the USA). A Fortis C18 column (2.1 × 100 mm, 1.7 μm) was used at 40°C. Water containing acetic acid (99.9/0.1, v/v, solvent A) and acetonitrile (solvent B) were used as mobile phase. A gradient of 0 min, 5% (B); 1 min, 25% (B); 3 min, 45% (B); 6 min, 95% (B); and 12 min, 95% (B) was used in both positive and negative mode. The posting time was set as 2 min. The injection volume and flow rate of the mobile phase were 5 μL and 0.3 ml/min, respectively. Electrospray ionization (ESI) with both negative and positive full scan was used for detection. Solutions were infused at 0.3 ml/min with the following parameters: temperature: 350°C, capillary: 4000 V, and speed of drying gas using nitrogen: 12 L/min. The samples for quality control (QC) were prepared by mixing all the serum samples from patients and injected six times before test for system stability checking and also injected every 10 samples during test.

Data and Statistical Analysis

The untargeted metabolomics was carried out as described previously (Sha et al., 2020). Briefly, deconvolution of LC-MS spectrum, including peak alignment, noise processing and baseline correction was performed using Thermo Data Analysis software. Compound Discoverer TM2.0 was then used for normalization to obtain the matrix. The raw intensities were transformed and normalized. For multiple peaks mapped to the same metabolites, the average intensity values were used. The matrix was then subjected to orthogonal partial least squares discrimination analysis (OPLS-DA) and principal component analysis (PCA) using the R ropls package (version 1.21.0) to obtain the differential metabolites between groups (Thevenot et al., 2015). Metabolites with variable importance in projection (VIP) > 1 were further analyzed by one-way analysis of variance (One-way ANOVA), followed by Benjamini-Hochberg correction and fold change analysis. Metabolites with fold change >2 or <0.5 and FDR <0.05 were considered to have statistically significant difference. Finally, the metabolites were traced to metabolite pathways through the Kyoto encyclopedia of genes and genomes (KEGG) by

TABLE 1 | Demographic and baseline disease characteristics of the patients.

Characteristic	SST group (N = 12)	Base line group (N = 14)	p Value
Age			ns
<45 yr	5	6	-
≥45 yr	7	8	-
ER status			ns
Positive	6	7	-
Negative	6	7	-
PR status			ns
Positive	7	8	-
Negative	5	6	-
Her-2 status			ns
Positive	4	5	-
Negative	8	9	-
Tumor size			ns
≤2 cm	2	3	-
>2 cm	10	11	-
Nodal status			ns
Positive	12	13	-
Negative	0	1	-
TNM stage			ns
Stage II	8	9	-
Stage III	4	5	-

Yr = years; p value was calculated using Chi-square test.

MetaboAnalyst (https://www.metaboanalyst.ca/MetaboAnalyst/home.xhtml) (Chong et al., 2018). All the statistics were performed using the R software (version 3.4.4).
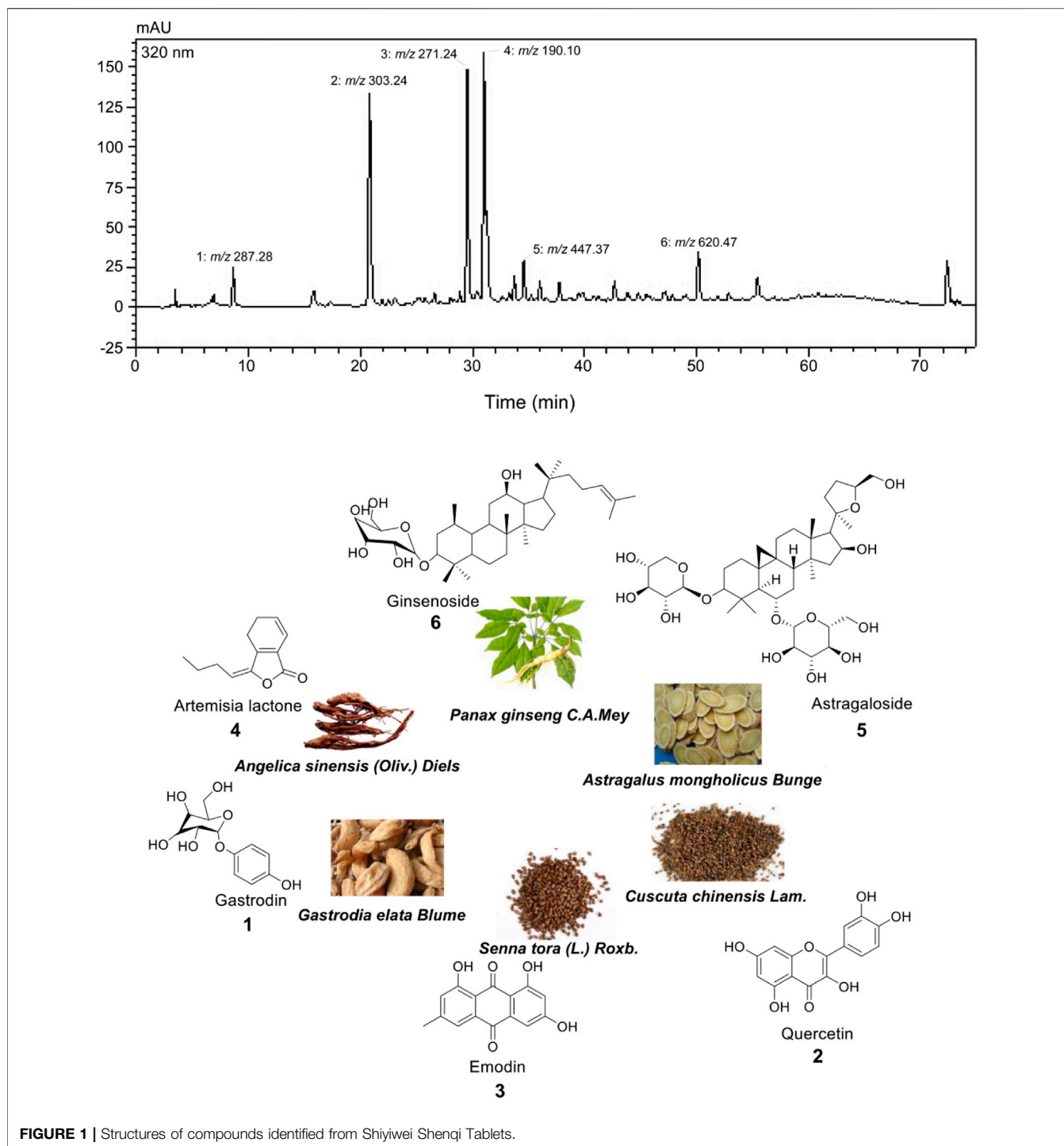
RESULTS

Identification of Key Compounds in SST

Serum samples from 30 breast cancer patients were used for untargeted metabolomics analysis. Among them, sample 1 and 3 from base-line chemotherapy and adjuvant SST treatment groups failed in untargeted metabolomics analysis due to their relatively low data quality. Baseline characteristics are presented in **Table 1**. The clinical characteristics including age, tumor TNM stage, tumor size, and PR, ER, HER2 and lymph node metastasis status showed no significant differences between the two groups to ensure the accuracy of this study. We used magnetic resonance imaging (MRI) to evaluate the efficacy of the two groups, and the results showed the SST group exhibited a better efficacy on breast cancer after a 14-day treatment (**Supplementary Figure S1**).

SST is mainly composed of eleven traditional Chinese medicine ingredients. Through our detection, we have found six key components including ginsenoside, artemisia iactone, astragaloside, gastrodin, emodin, and quercetin in SQEI by LC-HRMS (**Figure 1**). Therefore, we considered these six compounds as the main pharmaceutical components.

Untargeted Metabolomics Analysis of Serum Samples After Base Line Treatment

To confirm the stability of our HPLC-MS system, we performed PCA on the untargeted metabolomics data based on both
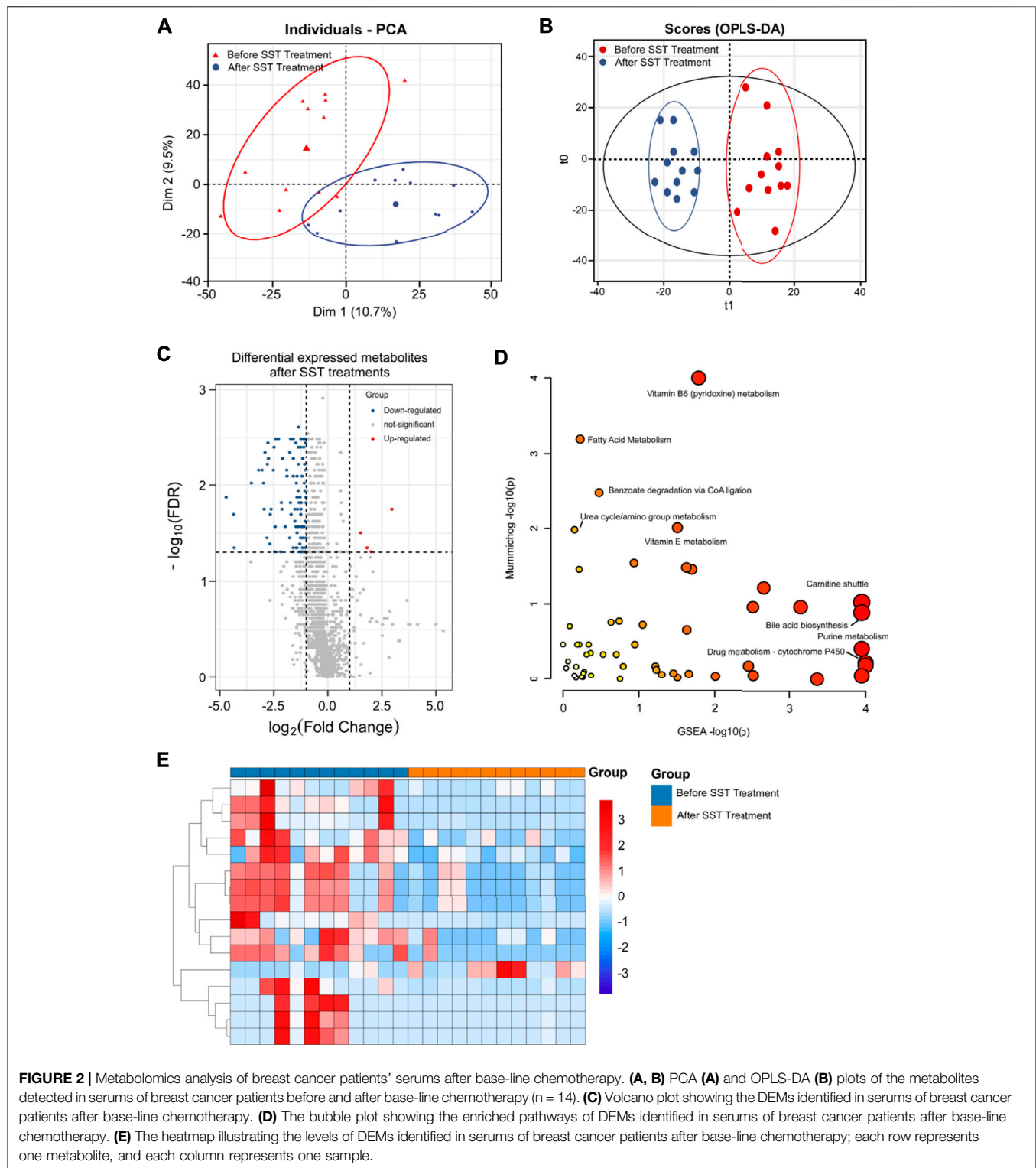
FIGURE 1 | Structures of compounds identified from Shiyiwei Shenqi Tablets.

positive and negative ion models. The results showed that the QC samples could be discriminated from the real samples in both positive and negative ion models. Furthermore, the QC samples tended to be clustered, which demonstrated the stability of our HPLC-MS system (**Supplementary Figure S2A**). We also calculated the relative standard deviation (RSD) of each metabolite identified. The results showed that the RSD values of different peaks of QC samples were small, further confirming

the stability of our HPLC-MS system (**Supplementary Figure S2B**).

We also performed untargeted metabolomics analysis using an HPLC-QE-Orbitrap-MS platform for 14 serum samples from breast cancer patients who received base line chemotherapy before surgery. Serum samples from patients before and after base line chemotherapy treatment were subjected to metabolomics analysis using an optimized HPLC-QE-

FIGURE 2 | Metabolomics analysis of breast cancer patients' serums after base-line chemotherapy. **(A, B)** PCA **(A)** and OPLS-DA **(B)** plots of the metabolites detected in serums of breast cancer patients before and after base-line chemotherapy (n = 14). **(C)** Volcano plot showing the DEMs identified in serums of breast cancer patients after base-line chemotherapy. **(D)** The bubble plot showing the enriched pathways of DEMs identified in serums of breast cancer patients after base-line chemotherapy. **(E)** The heatmap illustrating the levels of DEMs identified in serums of breast cancer patients after base-line chemotherapy; each row represents one metabolite, and each column represents one sample.

Orbitrap-MS method. The raw MS data of both negative and positive modes were imported into Thermo Data Analysis software for peak detection, correspondence, normalization and alignment. A data matrix was then subjected OPLS-DA and PCA using R ropls package. The PCA score plot

(**Figure 2A**) showed that serum samples after base line chemotherapy could be discriminated from those before base line chemotherapy (R2X = 0.526). Further OPLS-DA confirmed that serum samples after base line chemotherapy were clearly distinguished from those before base line chemotherapy

TABLE 2 | The representative differential metabolites identified in serum samples after base-line treatment.

Compound	m/z	R_t	Molecular formula	VIP	FC	FDR	Change	Metabolic pathway
1-(4Z,7Z,10Z,13Z,16Z,19Z-docosahexaenoyl)-sn-glycero-3-phosphocholine	567.3312	5.744	$C_{30}H_{50}NO_7P$	2.023	0.252	0.0014	Down	Phospholipid metabolism
1-[(11Z,14Z)]-icosadienoyl-sn-glycero-3-phosphocholine	547.3628	6.401	$C_{28}H_{54}NO_7P$	2.006	0.426	0.0022	Down	Phospholipid metabolism
1-[(8Z,11Z,14Z)-icosatrienoyl]-sn-glycero-3-phosphocholine	545.3476	6.131	$C_{28}H_{52}NO_7P$	1.110	0.470	0.0468	Down	Phospholipid metabolism
1-[(9Z)-hexadecenoyl]-sn-glycero-3-phosphocholine	493.3160	5.68	$C_{24}H_{48}NO_7P$	1.596	0.430	0.0261	Down	Phospholipid metabolism
Ala-Pro	186.1001	0.688	$C_8H_{14}N_2O_3$	1.232	4.006	0.0152	Up	Amino acid metabolism
Gly-Pro	172.0848	0.79	$C_7H_{12}N_2O_3$	1.375	2.656	0.0152	Up	Amino acid metabolism
H-Gly-Pro-Pro-OH	269.1370	0.877	$C_{12}H_{19}N_3O_4$	1.208	3.268	0.0261	Up	Amino acid metabolism
leu-leu-leu-leu	470.3460	2.624	$C_{24}H_{46}N_4O_5$	1.792	0.276	0.0019	Down	Amino acid metabolism
Linoleamide	279.2556	6.829	$C_{18}H_{33}NO$	1.339	0.382	0.0082	Down	Fatty acid metabolism
Methyl L-leucyl-L-leucinate	258.1939	2.429	$C_{13}H_{26}N_2O_3$	1.785	0.217	0.0026	Down	Amino acid metabolism
N5-Ethyl-L-glutamine	174.1004	1.706	$C_7H_{14}N_2O_3$	1.547	2.301	0.0082	Up	Amino acid metabolism
N-Acetyl-D-alloisoleucine	173.1044	2.816	$C_8H_{15}NO_3$	1.759	2.403	0.0026	Up	Amino acid metabolism
N-Acetyl-DL-norvaline	159.0886	2.227	$C_7H_{13}NO_3$	1.834	2.234	0.0011	Up	Amino acid metabolism
PC	757.5612	13.71	$C_{42}H_{80}NO_8P$	1.987	0.406	0.0064	Down	Phospholipid metabolism
Val-Arg	273.1799	2.594	$C_{11}H_{23}N_5O_3$	1.041	2.604	0.0173	Up	Amino acid metabolism
[FAtrihydroxy(18:0)]9_10_13-trihydroxy-11-octadecenoicacid	330.2402	4.596	$C_{18}H_{34}O_5$	1.639	0.356	0.0046	Down	Fatty acid metabolism
[FA(18:4)]6Z_9Z_12Z_15Z-octadecatetraenoicacid	276.2083	5.782	$C_{18}H_{28}O_2$	1.813	0.433	0.0040	Down	Fatty acid metabolism
[FAhydroxy(20:4)]5S-hydroxy-12-keto-6Z_8E_10E_14Z-eicosatetraenoicacid	334.2132	7.307	$C_{20}H_{30}O_4$	1.942	0.172	0.0011	Down	Fatty acid metabolism
(Dichloromethyl)phosphonate	161.9056	0.656	$CHCl_2O_3P$	1.642	0.203	0.0298	Down	Phospholipid metabolism
Val-Leu-Gly-Lys	415.2773	2.575	$C_{19}H_{37}N_5O_5$	1.171	2.502	0.0229	Up	Amino acid metabolism

(**Figure 2B**), and the Q2Y and R2Y values were 0.883 and 0.984, respectively.
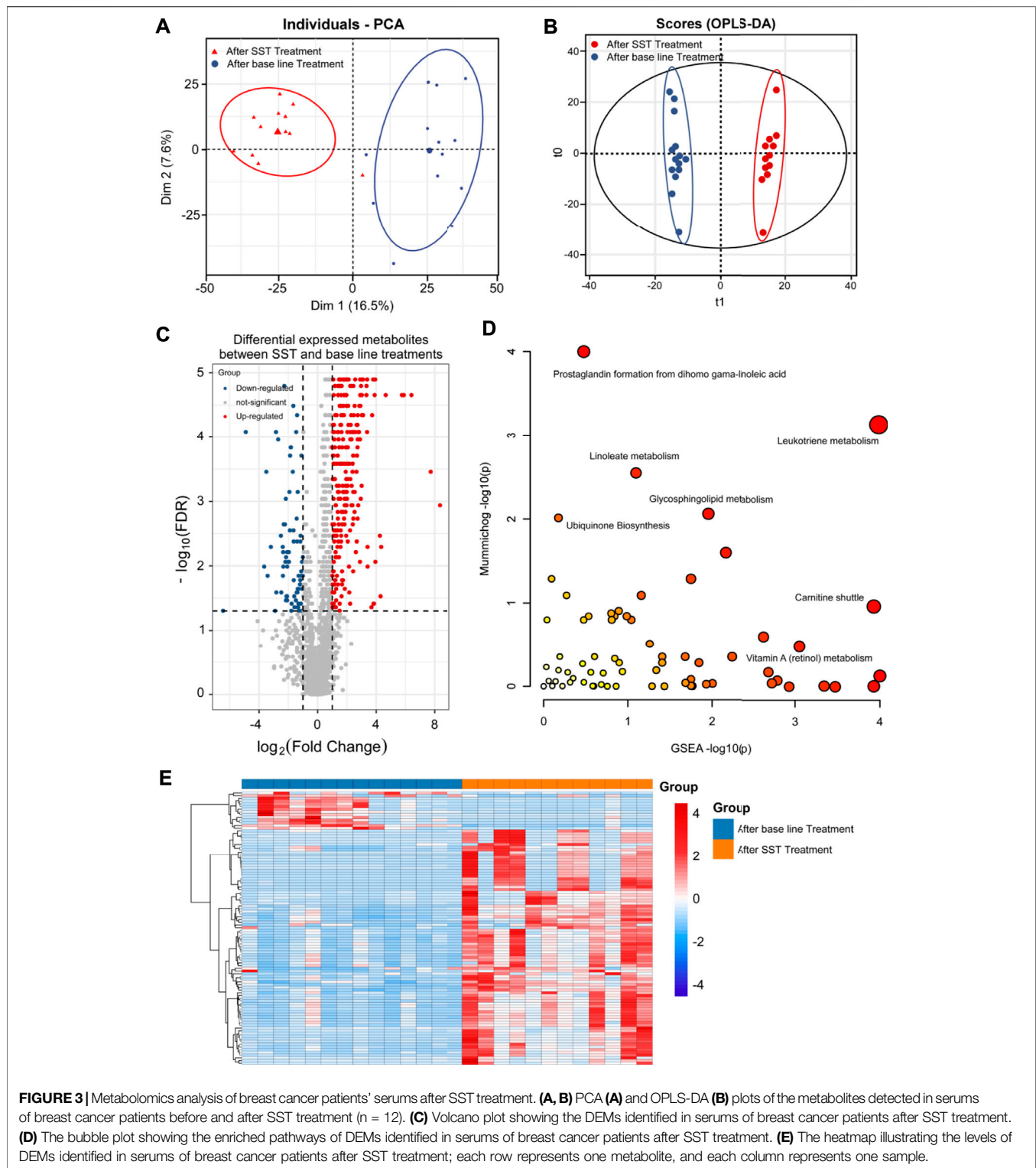
VIP, which is frequently used in metabolomic analysis, was employed to identify the differentially expressed metabolites (DEMs) after treatments. High-resolution MS peaks were annotated to known metabolites by Thermo Data Analysis software according to the database including HMDB, KEGG, and in-house reference metabolites. The VIP score and fold change for each metabolite before and after treatments were then calculated. In total, 186 metabolites including 41 up-regulated and 145 down-regulated metabolites showed significant changes after treatments (**Figure 2C and 2E**, FDR <0.05 and fold change >2 or <0.5 and VIP >1) (the complete DEMs list is shown in **Supplementary Table S1**). The DEMs included amino acid, fatty acids and phospholipids, such as 1-[(9Z)-hexadecenoyl]-sn-glycero-3 -phosphocholine, [FA (18:4)] 6Z_9Z_12Z_15Z-octadecatetraenoic acid, Ala-Pro, and Gly-Pro (**Table 2**).

The changes of metabolic pathways were analyzed using MetaboAnalyst webtool, and the results showed that the potential metabolic pathways related to base line chemotherapy were those involved in metabolism of amino acids, fatty acids, and vitamins. In particular, pathways involved in metabolism of glycosphingolipid, linoleate, and leukotriene, and carnitine shuttle were considered the most probably involved metabolic pathways after base line chemotherapy (**Figure 2D** and **Supplementary Table S2**).

Untargeted Metabolomics Analysis of Patient Serums After SST Treatment

Untargeted metabolomics analysis of patient serum samples was conducted using HPLC-QE-Orbitrap-MS platform. After peak detection, alignment, correspondence, and normalization, the PCA score plot showed that the serum samples after SST treatment could be distinguished from those before SST treatment (**Figure 3A**, R^2X = 0.540). Further OPLS-DA confirmed that serum samples after SST treatment were clearly discriminated from those before SST treatment, and the R^2Y and Q^2Y values were 0.921 and 0.583, respectively (**Figure 3B**).

FIGURE 3 | Metabolomics analysis of breast cancer patients' serums after SST treatment. **(A, B)** PCA **(A)** and OPLS-DA **(B)** plots of the metabolites detected in serums of breast cancer patients before and after SST treatment (n = 12). **(C)** Volcano plot showing the DEMs identified in serums of breast cancer patients after SST treatment. **(D)** The bubble plot showing the enriched pathways of DEMs identified in serums of breast cancer patients after SST treatment. **(E)** The heatmap illustrating the levels of DEMs identified in serums of breast cancer patients after SST treatment; each row represents one metabolite, and each column represents one sample.

To identify the DEMs after SST treatment, the high-resolution MS peaks of the LC-MS chromatograms were annotated to known candidates by Thermo Data Analysis software according to the database including HMDB, KEGG, and in-house reference metabolites. The VIP score for each metabolite was then calculated by combing the peaks mapped to one metabolite. Totally 76 down-regulated and 3 up-regulated metabolites exhibited significant changes after SST treatment (**Figure 3C and 3E**, FDR <0.05 and fold change >2 or <0.5 and VIP >1) (the complete DEMs list is shown in **Supplementary**

TABLE 3 | The representative differential metabolites identified in serum samples after SST treatment.

Compound	m/z	R_t	Molecular formula	VIP	FC	FDR	Change	Metabolic pathway
His-Trp	341.1479	1.815	$C_{17}H_{19}N_5O_3$	1.594	7.792	0.018	Up	Amino acid metabolism
Cystathionine	222.0672	2.883	$C_7H_{14}N_2O_4S$	2.110	0.109	0.007	Down	Amino acid metabolism
Adenosine	267.0962	0.872	$C_{10}H_{13}N_5O_4$	1.695	0.141	0.035	Down	Nucleotide metabolism
Histidinate	154.0620	2.086	$C_6H_8N_3O_2$	1.411	0.205	0.003	Down	Amino acid metabolism
Arg-Phr	321.1790	1.025	$C_{15}H_{23}N_5O_3$	1.560	0.427	0.015	Down	Amino acid metabolism
Deoxycholic Acid	392.2926	6.832	$C_{24}H_{40}O_4$	1.818	0.496	0.015	Down	Bile acid metabolism
L-Phe-L-Phe	312.1470	3.003	$C_{18}H_{20}N_2O_3$	1.581	4.004	0.049	Up	Amino acid metabolism
D-Ala-D-Ala	160.0847	1.956	$C_6H_{12}N_2O_3$	1.502	0.495	0.013	Down	Amino acid metabolism
Adenine	135.0546	2.029	$C_5H_5N_5$	2.142	0.488	0.004	Down	Nucleotide metabolism
DL-α-Aminocaprylic acid	159.1259	2.720	$C_8H_{17}NO_2$	1.365	0.396	0.015	Down	Amino acid metabolism

Table S3). Interestingly, two dipeptides His-Trp and L-Phe-L-Phe were significantly up-regulated in serum after SST treatment (**Table 2**). In contrast, several metabolites involved in metabolism of nucleotides such as adenine and adenosine were dramatically down-regulated after SST treatment (**Table 3**).

We further analyzed the alterations of metabolic pathways after SST treatment using the MetaboAnalyst web tool. As shown in **Figure 3D** and **Supplementary Table S4**, the changes of metabolic pathways were mainly involved in metabolism of Vitamin B6 (pyridoxine), Vitamin E, and purine, carnitine shuttle, biosynthesis of bile acid, and regulation of drug metabolism-cytochrome P450. The scatter plot displayed the most possible metabolic pathways *via* circle size. Therefore, the metabolism of Vitamin B6 and purine, and carnitine shuttle were considered to have most altered metabolic pathways after SST treatment.

Untargeted Metabolomics Analysis of Patient Serum Between SST Treatment and Base Line Chemotherapy

Since dramatic metabolic changes happened after SST treatment and base line chemotherapy, we next analyzed and compared these metabolic alterations between patients who received SST treatment or only base line chemotherapy. The PCA score plot clearly separated patients receiving SST treatment from those receiving base line chemotherapy based on the serum metabolomics data (**Figure 4A**, $R^2X = 0.522$). The OPLS-DA results further demonstrated that serum samples after SST treatment were clearly discriminated from those after base line chemotherapy, the R^2Y and Q^2Y values were 0.898 and 0.655, respectively (**Figure 4B**).

DEMs were also identified by the VIP score of each metabolite. A total of 287 metabolites including 50 down-regulated and 237 up-regulated metabolites exhibited significant changes in serum between SST and base line chemotherapy treatments (**Figure 4C and 4E**, FDR <0.05 and fold change >2 or <0.5 and VIP >1) (the complete DEMs list is shown in **Supplementary Table S5**). In particular, metabolites such as phospholipids, amino acids, and fatty acids showed significant changes between SST and base line chemotherapy treatments (**Table 4**). The metabolic pathway changes between SST and

base line chemotherapy treatments were further analyzed using the MetaboAnalyst web tool. As shown in **Figure 4D** and **Supplementary Table S6**, metabolic pathways involved in carnitine shuttle, saturated fatty acids beta-oxidation, parathio degradation, bile acid biosynthesis, and leukotriene metabolism were considered the most altered metabolic pathways between SST and base line chemotherapy treatments.
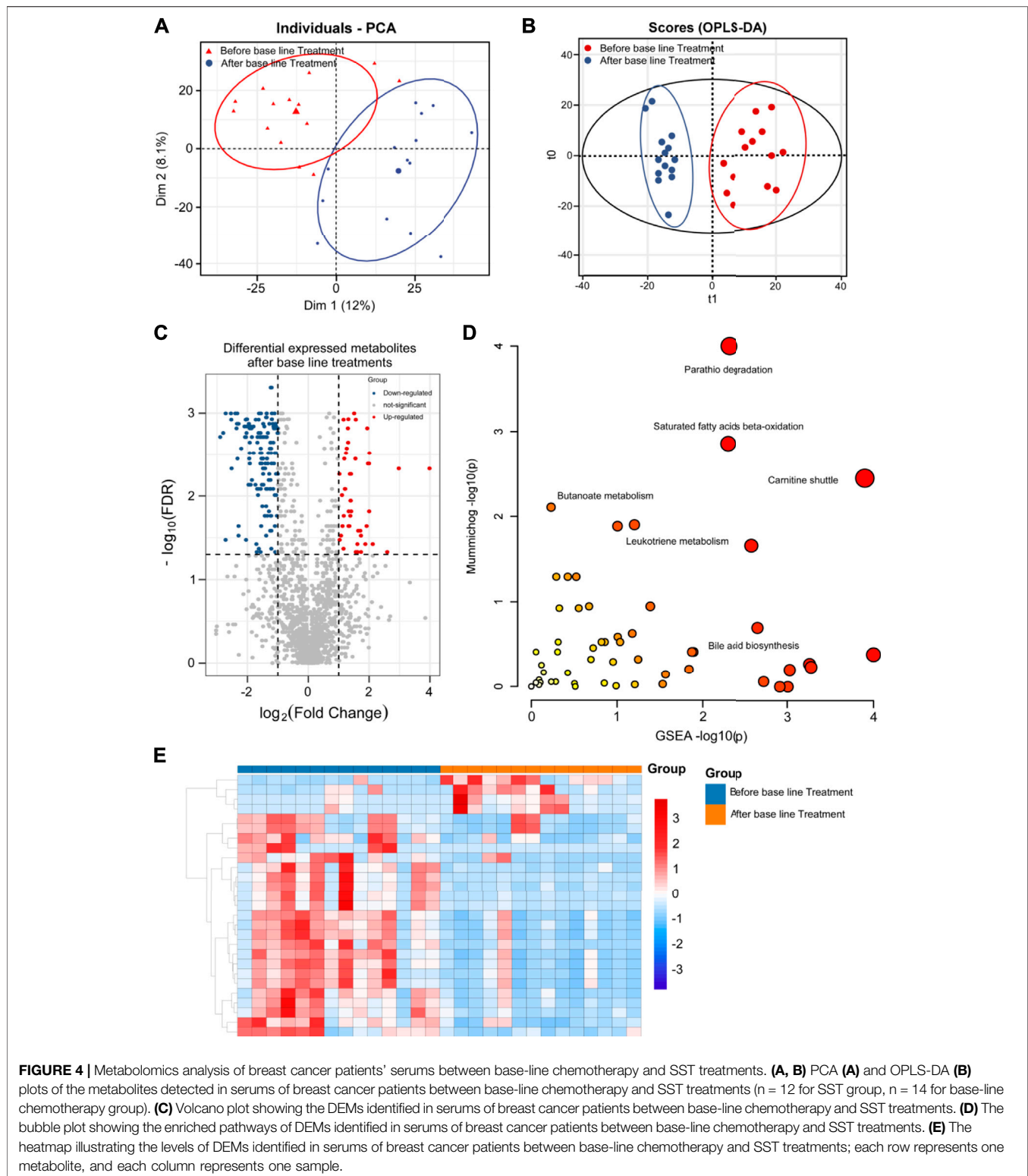
Amino Acid Metabolism Was Identified as an Important Pathway After SST Treatment by Untargeted Metabolomics Analysis

Amino acid metabolism enhances tumor cell proliferation survival by supporting building block synthesis, producing immunosuppressive metabolites for immune escape, and reducing the production of agents mitigating oxidative stress (Pavlova and Thompson, 2016; Tabe et al., 2019). At the same time, numerous short peptides are generated during cancer initiation and progression. Untargeted metabolomics analysis results revealed that many short peptides such as val-pro-gly-val-gly, tyr-lys-pro-asn, and D-Ala-D-Ala were dramatically reduced after SST treatment, while these metabolites remained unchanged after base line chemotherapy (**Figure 5A**). In addition, some amino acids including N-Acetyl-L-Carnosine and arginine were also significantly reduced after SST treatment (**Figure 5A**). Intriguingly, the dipeptide his-trp was significantly increased after SST treatment, indicating SST treatment might induce the expression of some protective peptides (**Figure 5A**). Furthermore, some nucleotides such as adenine and adenosine were dramatically decreased after SST treatment compared with those after base line chemotherapy. These results showed that SST may exert its effect in breast cancer treatment through modulating amino acid metabolism.

Glycometabolism Pathways Were Demonstrated as Co-regulatory Pathways in Both SST and Base Line Chemotherapy Treatments by Untargeted Metabolomics Analysis

Glycometabolism pathways including the tricarboxylic acid (TCA) cycle and glycolysis are reported to play important

FIGURE 4 | Metabolomics analysis of breast cancer patients' serums between base-line chemotherapy and SST treatments. **(A, B)** PCA **(A)** and OPLS-DA **(B)** plots of the metabolites detected in serums of breast cancer patients between base-line chemotherapy and SST treatments (n = 12 for SST group, n = 14 for base-line chemotherapy group). **(C)** Volcano plot showing the DEMs identified in serums of breast cancer patients between base-line chemotherapy and SST treatments. **(D)** The bubble plot showing the enriched pathways of DEMs identified in serums of breast cancer patients between base-line chemotherapy and SST treatments. **(E)** The heatmap illustrating the levels of DEMs identified in serums of breast cancer patients between base-line chemotherapy and SST treatments; each row represents one metabolite, and each column represents one sample.

roles including promoting proliferation, growth, and long-term maintenance in carcinogenesis. (Pavlova and Thompson, 2016; Martinez-Outschoorn et al., 2017). The common characteristics of cancer cells known as Warburg Effect include enhancing

uptake of glucose and glucose fermentation to lactate. Normal cells mainly produce energy through glycolysis, followed by TCA cycle and oxidative phosphorylation (Vander Heiden et al., 2009). However, cancer cells principally produce their energy through

TABLE 4 | The representative differential metabolites identified in serum samples between SST treatment and base-line treatment.

Compound	m/z	R_t	Molecular formula	VIP	FC	FDR	Change	Metabolic pathway
leu-leu-leu-leu	470.346	2.624	$C_{24}H_{46}N_5$	1.912	7.464	0.0001	Up	Amino acid metabolism
LysoPC(20:5(5Z,8Z,11Z,14Z,17Z))	541.3163	5.445	$C_{28}H_{48}N_7P$	1.559	5.797	0.0007	Up	Phospholipid metabolism
LysoPC(22:4(7Z,10Z,13Z,16Z))	571.3629	6.335	$C_{30}H_{54}N_7P$	1.670	2.926	0.0009	Up	Phospholipid metabolism
LysoPC(22:5(7Z,10Z,13Z,16Z,19Z))	569.347	6.013	$C_{30}H_{52}N_7P$	1.651	3.764	0.0009	Up	Phospholipid metabolism
N5-Ethyl-L-glutamine	174.1004	1.706	$C_7H_{14}N_{23}$	1.440	0.496	0.0073	Down	Amino acid metabolism
N-Acetyl-L-methionine	191.0612	2.264	$C_7H_{13}NOS$	1.285	0.447	0.0034	Down	Amino acid metabolism
N-Acetyl-L-tyrosine	223.0841	2.173	$C_{11}H_{13}N_4$	1.496	0.464	0.0001	Down	Amino acid metabolism
Omega	321.2144	5.143	$C_{15}H_{31}N_6$	1.180	3.107	8.23E-	Up	Fatty acid metabolism
PC	757.5612	13.71	$C_{42}H_{80}N_8P$	1.671	2.589	0.0014	Up	Phospholipid metabolism
Pyrimidine	80.03746	11.15	$C_4H_4N_2$	1.665	1.420	0.0018	Up	Nucleotide metabolism
Stearic acid	284.2714	8.208	$C_{18}H_{36}O_2$	1.569	1.800	0.0050	Up	Fatty acid metabolism
Ubiquinone-1(CoQ1)	250.1202	5.035	$C_{14}H_{18}O_4$	1.589	1.450	0.0014	Up	Energy metabolism
val-leu-gly-lys	415.2774	2.575	$C_{19}H_{37}N_5$	1.045	0.271	0.0001	Down	Amino acid metabolism
[FA(16:2)]N-hexadecyl-ethanolamine	299.2819	5.945	$C_{18}H_{37}NO_2$	1.393	2.191	0.0004	Up	Fatty acid metabolism
[FA(18:2)]9Z_11E-octadecadienoicacid	280.2399	6.174	$C_{18}H_{32}O_2$	1.713	1.846	0.0005	Up	Fatty acid metabolism
[FA(18:4)]6Z_9Z_12Z_15Z-octadecatetraenoicacid	276.2084	5.782	$C_{18}H_{28}O_2$	1.669	3.871	0.0001	Up	Fatty acid metabolism
Ala-Pro	186.1001	0.688	$C_8H_{14}N_2O_3$	1.292	0.154	0.0001	Down	Amino acid metabolism
Arachidonic acid	304.2401	7.147	$C_{20}H_{32}O_2$	1.294	1.293	0.0086	Up	Fatty acid metabolism
asp-gly-lys	318.153	0.587	$C_{12}H_{22}N_6$	1.500	6.844	0.0011	Up	Amino acid metabolism
Creatine	131.0697	0.706	$C_4H_9N_3O_2$	1.234	1.458	0.0034	Up	Amino acid metabolism
Creatinine	113.0591	2.904	$C_4H_7N_3O$	1.581	1.860	0.0073	Up	Amino acid metabolism
Gly-Pro	172.0849	0.79	$C_7H_{12}N_{23}$	1.173	0.415	0.0495	Down	Amino acid metabolism
Lauryl glucoside	348.2507	4.264	$C_{18}H_{36}O_6$	1.237	1.522	0.0258	Up	Glycometabolism

enhanced glycolysis, followed by lactic acid fermentation in the presence of abundant oxygen in microenvironment. Interestingly, citric acid and L-(+)-lactic acid were dramatically upregulated after both SST and base line chemotherapy treatments (**Figure 6**). Together, these upregulations may have resulted from cancer cells that are killed by chemotherapy or SST.

DISCUSSION

Nowadays, surgery combined with radiotherapy, chemotherapy, targeted therapy, hormonal therapy, and immunotherapy has been extensively used for treating patients with breast cancer (Harbeck et al., 2019). Chemotherapy is commonly used for treatment of different stages of breast cancer. Moreover, neoadjuvant chemotherapy has been used to shrink tumors before surgery (Early Breast Cancer Trialists' Collaborative Group (EBCTCG), 2018; Untch et al., 2014). Normally, the chemotherapeutic strategy is established by combining two or more agents to achieve a better effect for breast cancer. Although chemotherapy shows significant efficacy in killing cancer cells, it also results in non-negligible side effects such as alopecia, vomiting, constipation, diarrhea, immune dysfunction, and myelosuppression (Tao et al., 2015). The severity of these adverse effects is highly related to the regimen type, drug dosage, treatment length, and general health of patients. Furthermore, some breast cancer patients also show significant chemotherapy resistance. Thus, an adjuvant treatment aimed at managing side effects and increasing chemotherapy sensitivity is expected.

TCM has been increasingly combined with regular chemotherapy in breast cancer treatment because it can enhance chemotherapy sensitivity and alleviate the side effects induced by chemotherapy (Li et al., 2020). Some meta-analyses and systematic reviews have shown that the adjuvant use of TCM with chemotherapy can attenuate a series of side effects induced by chemotherapy including alopecia, vomiting, diarrhea, constipation, myelosuppression, and immune dysfunction (Li et al., 2020). For example, previous studies have shown that a TCM named Yiqi Jianpi Hewei could alleviate the occurrence rate of chemotherapy induced constipation in breast cancer patients (Wu et al., 2019; Li et al., 2020). The SST has been used to restore the immune function of chemotherapeutic or post-operational period gastric cancer patients (Lu et al., 2020). However, the mechanisms of pharmacodynamics and drug-drug interaction remain unclear. Moreover, the impacts of compounds on drug metabolism is not just simply the sum of effects from individual compounds.

In this study, we applied an untargeted metabolomics analysis method using HPLC-MS to examine the metabolite changes in serum of breast cancer patients following base line chemotherapy and SST adjuvant therapy. In addition, the mass spectrometry analysis data were further subjected to OPLS-DA and PCA analyses to obtain good division. Numerous differentially expressed metabolites especially those involved in fatty acid or amino acid metabolism have been identified after base line chemotherapy and SST adjuvant therapy, and treatments had shown significant impacts on the metabolites. We also analyzed the metabolic pathways involved based on the differentially expressed metabolites. The carnitine shuttle, bile acid biosynthesis, drug metabolism-cytochrome P450, and vitamin B6 (pyridoxine), Vitamin E, and purine metabolism pathways were considered as the potential pathways affected by SST treatment.
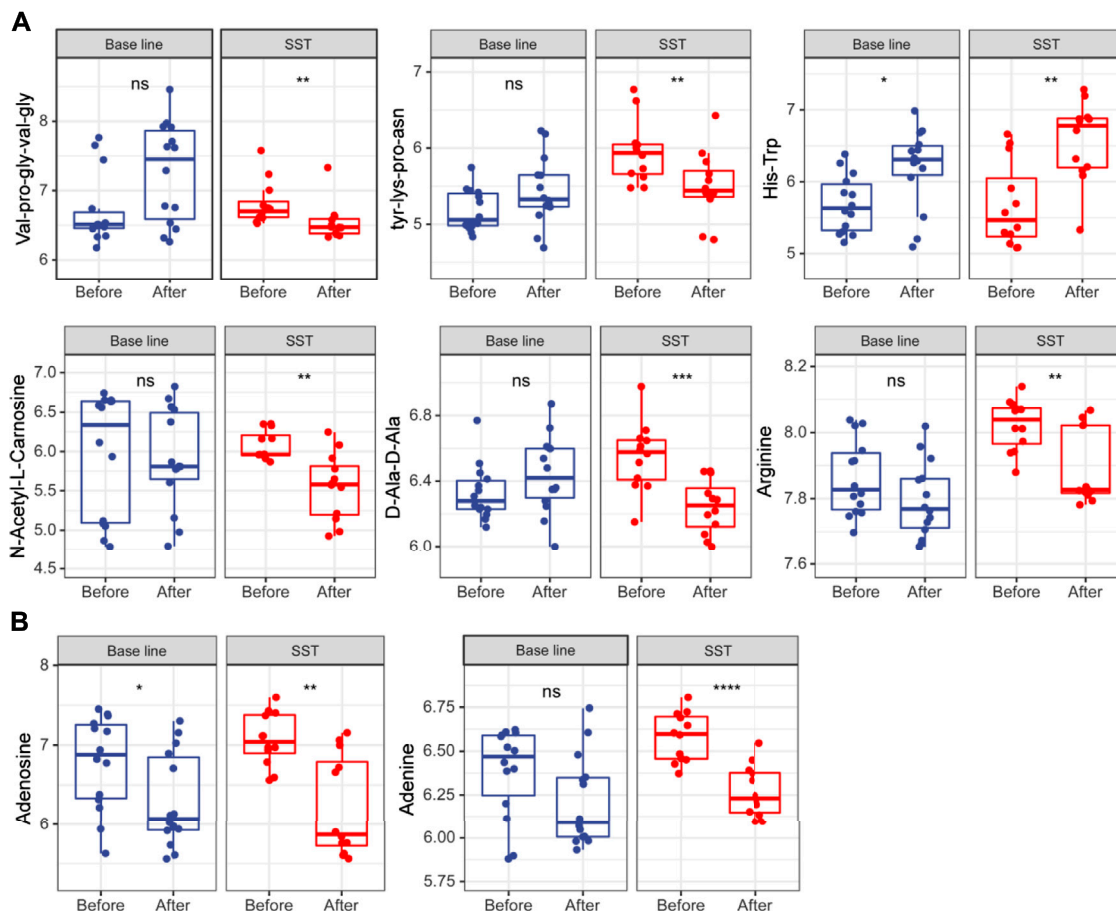
FIGURE 5 | Levels of amino acid **(A)** and nucleotide **(B)** metabolism related metabolites in serums of breast cancer patients receiving base-line chemotherapy or adjuvant SST treatment; ns, not significant; *p < 0.05, **p < 0.01, ***p < 0.001, and ****p < 0.0001 by student's t test.
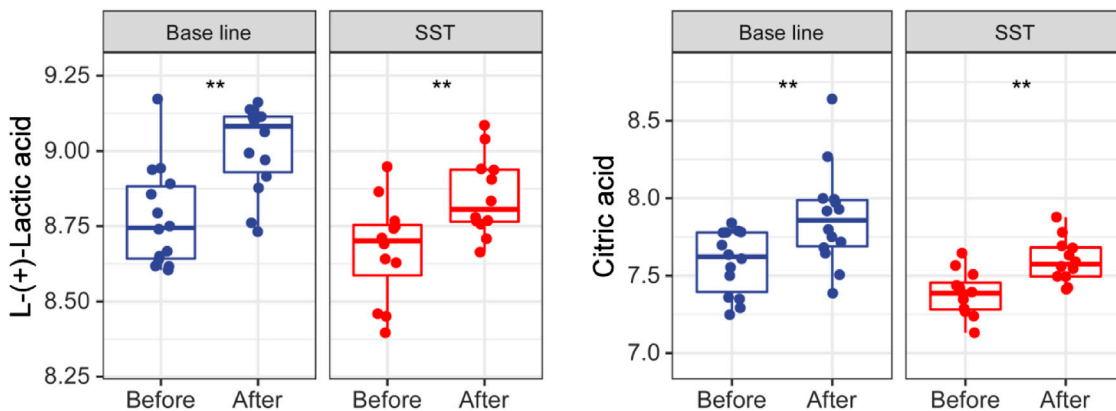
FIGURE 6 | Levels of glucose metabolism related metabolites in serums of breast cancer patients receiving base-line chemotherapy or adjuvant SST treatment. **p < 0.01 by student's t test.

Amino acid metabolic disorder plays acritical role in breast cancer (Pavlova and Thompson, 2016; Tabe et al., 2019). The differentially expressed metabolites we found, such as val-pro-gly-val-gly, tyr-lys-pro-asn, and D-Ala-D-Ala were significantly reduced after adjuvant SST treatment. In breast cancer initiation and progression, many peptides called neoantigens are generated

by disrupted alternative splicing processes and gene mutations (Benvenuto et al., 2019). In addition, amino acid metabolism disruption also leads to aberrant expression of short peptides in cancer. In this study, a lot of short peptides were detected with a remarkable decrease in breast cancer patients after adjuvant SST treatment. This result means that adjuvant SST treatment can inhibit the production of potential neoantigens, thereby alleviating tumor burden by affecting the amino acid metabolism disorder. Warburg effect has been known as an important phenomenon in cancer development: different from normal cells which primarily use oxidative phosphorylation in mitochondria to generate energy, most cancer cells primarily use aerobic glycolysis to obtain energy for development. We found the differential metabolites were all involved in aerobic glycolysis, such as L-(+)-lactic acid and citric acid, suggesting that the adjuvant SST treatment can improve the prognosis of breast cancer, thereby affect the glucose metabolism disorder.

We systematically performed untargeted metabolic analysis to investigate the potential mechanism of SST in breast cancer treatment. The results revealed that SST may enhance chemotherapy sensitivity and alleviate side-effects mainly by affecting the amino acid and glucose metabolism pathways. However, the detailed mechanisms of how SST impacts the cancer cell malignant biological properties remain further study. Furthermore, SST led to significant alleviation of side effects induced by chemotherapy, which may be related to drug and vitamin metabolism pathways. Hypothetically, SST may protect patients from vomiting and aspirating gastric contents through affecting the patients' gut microbiota, thereby influencing the secondary metabolites.

At present, although TCM has been widely applied in breast cancer therapy for many years in China and also some other Asian counties (Xiang et al., 2019), it remains a challenge to introduce TCM to western countries. Currently, most reported clinical trials about the use of TCM in treating breast cancer were performed in Chinese patients. Therefore, more clinical trials are needed to be performed in western countries to facilitate the use of TCM worldwide. Another concern is whether TCM influences the pharmacokinetics of chemotherapeutic agents in combination treatments. Some *in vivo* studies showed that there were no interactions between chemotherapeutic agents and TCM such as berberine. However, pharmacokinetic studies of chemotherapeutic agents in combination with TCM are quite few. Moreover, the mechanisms about how TCM alleviates the side-effects induced by chemotherapy also need further research.

CONCLUSION

We used an HPLC-MS-based untargeted metabolomics analysis method to investigate drug interactions between base line chemotherapy and SST treatment. Based on the HPLC-MS results, we have identified several differential metabolites after base line chemotherapy and SST treatment, respectively. The metabolites exhibited different changes before and after treatment of only base line chemotherapy or combination treatment with SST, indicating that the SST treatment can affect the glycometabolism, fatty acid, bile acid and amino acid metabolism. Especially, some short peptides which are potential tumor neoantigens were significantly reduced after adjuvant SST treatment. This work has elucidated the interaction mechanism between base line chemotherapy and SST treatment based on analysis of metabolite changes, and identified potential metabolic pathways involved, which might shed new light on clinical medication.

DATA AVAILABILITY STATEMENT

The original contributions presented in the study are included in the article/**Supplementary Material**, further inquiries can be directed to the corresponding authors.

ETHICS STATEMENT

The studies involving human participants were reviewed and approved by The Fourth Affiliated Hospital of Anhui Medical University. The patients/participants provided their written informed consent to participate in this study.

AUTHOR CONTRIBUTIONS

HW, YZ, JP, QS, and YG performed the experiments and participated in article writing. HW, YG, QS, and YZ designed and performed the bioinformatic data analyses. HW, XX, XYa, and AL collected the clinical samples. XM, AX, WW, and TG interpreted the results. XYu, WW, YG, and GL provided help for statistical analyses. YG, XH, WL, and ZW revised the article. All authors contributed to the article and approved the submitted version.

FUNDING

SUPPLEMENTARY MATERIAL

The Supplementary Material for this article can be found online at: https://www.frontiersin.org/articles/10.3389/fphar.2021.720886/full#supplementary-material

REFERENCES

Alonso, A., Marsal, S., and Julià, A. (2015). Analytical Methods in Untargeted Metabolomics: State of the Art in 2015. *Front. Bioeng. Biotechnol.* 3, 23. doi:10.3389/fbioe.2015.00023

Benvenuto, M., Focaccetti, C., Izzi, V., Masuelli, L., Modesti, A., and Bei, R. (2021). Tumor Antigens Heterogeneity and Immune Response-Targeting Neoantigens in Breast Cancer. *Semin. Cancer Biol.* 72, 65–75. doi:10.1016/j.semcancer.2019.10.023

Cao, W., Chen, H. D., Yu, Y. W., Li, N., and Chen, W. Q. (2021). Changing Profiles of Cancer burden Worldwide and in China: a Secondary Analysis of the Global Cancer Statistics 2020. *Chin. Med. J. (Engl)* 134, 783–791. doi:10.1097/CM9.0000000000001474

Chen, W., Zheng, R., Baade, P. D., Zhang, S., Zeng, H., Bray, F., et al. (2016). Cancer Statistics in China, 2015. *CA Cancer J. Clin.* 66, 115–132. doi:10.3322/caac.21338

Chen, Y. Z., Lin, F., Zhuang, G. B., Ren, Y., and Li, P. P. (2011). Protective Effect of Renshen Yangrong Decoction (人参养荣汤) on Bone Marrow against Radiation Injury in Mouse. *Chin. J. Integr. Med.* 17, 453–458. doi:10.1007/s11655-011-0634-1

Chong, J., Soufan, O., Li, C., Caraus, I., Li, S., Bourque, G., et al. (2018). MetaboAnalyst 4.0: towards More Transparent and Integrative Metabolomics Analysis. *Nucleic Acids Res.* 46, W486–W494. doi:10.1093/nar/gky310

Cui, L., Lu, H., and Lee, Y. H. (2018). Challenges and Emergent Solutions for LC-MS/MS Based Untargeted Metabolomics in Diseases. *Mass. Spectrom. Rev.* 37, 772–792. doi:10.1002/mas.21562

DeSantis, C. E., Ma, J., Gaudet, M. M., Newman, L. A., Miller, K. D., Goding Sauer, A., et al. (2019). Breast Cancer Statistics, 2019. *CA Cancer J. Clin.* 69, 438–451. doi:10.3322/caac.21583

Dong, J., Su, S. Y., Wang, M. Y., and Zhan, Z. (2010). Shenqi Fuzheng, an Injection Concocted from Chinese Medicinal Herbs, Combined with Platinum-Based Chemotherapy for Advanced Non-small Cell Lung Cancer: a Systematic Review. *J. Exp. Clin. Cancer Res.* 29, 137. doi:10.1186/1756-9966-29-137

Early Breast Cancer Trialists' Collaborative Group (EBCTCG) (2018). Long-term Outcomes for Neoadjuvant versus Adjuvant Chemotherapy in Early Breast Cancer: Meta-Analysis of Individual Patient Data from Ten Randomised Trials. *Lancet Oncol.* 19, 27–39. doi:10.1016/S1470-2045(17)30777-5

Fang, T., Yan, Y. X., Yang, Y., Lv, Y. X., Chang, Q. Q., and Zhang, D. D. (2020). Ethyl Acetate Fraction from Hedyotis Diffusa Plus Scutellaria Barbata Suppresses Migration of Bone-Metastatic Breast Cancer Cells via OPN-FAK/ERK/NF-κB Axis. *Evid. Based Complement. Alternat Med.* 2020, 3573240. doi:10.1155/2020/3573240

Guo, M. Z., Wang, T. Y., Yang, J., Chang, H., Ji, S., and Tang, D. Q. (2019). Interaction of Clopidogrel and Fufang Danshen Dripping Pills Assay in Coronary Heart Disease Based on Non-target Metabolomics. *J. Ethnopharmacol* 234, 189–196. doi:10.1016/j.jep.2019.01.030

Harbeck, N., Penault-Llorca, F., Cortes, J., Gnant, M., Houssami, N., Poortmans, P., et al. (2019). Breast Cancer. *Nat. Rev. Dis. Primers* 5, 66. doi:10.1038/s41572-019-0111-2

Jang, C., Chen, L., and Rabinowitz, J. D. (2018). Metabolomics and Isotope Tracing. *Cell* 173, 822–837. doi:10.1016/j.cell.2018.03.055

Johnson, C. H., Ivanisevic, J., and Siuzdak, G. (2016). Metabolomics: beyond Biomarkers and towards Mechanisms. *Nat. Rev. Mol. Cel Biol* 17, 451–459. doi:10.1038/nrm.2016.25

Kalwat, M. A., and Cobb, M. H. (2017). Mechanisms of the Amplifying Pathway of Insulin Secretion in the β Cell. *Pharmacol. Ther.* 179, 17–30. doi:10.1016/j.pharmthera.2017.05.003

Li, B., He, X., Jia, W., and Li, H. (2017). Novel Applications of Metabolomics in Personalized Medicine: A Mini-Review. *Molecules* 22, 1173. doi:10.3390/molecules22071173

Li, S., So, T. H., Tang, G., Tan, H. Y., Wang, N., Ng, B. F. L., et al. (2020). Chinese Herbal Medicine for Reducing Chemotherapy-Associated Side-Effects in Breast Cancer Patients: A Systematic Review and Meta-Analysis. *Front. Oncol.* 10, 599073. doi:10.3389/fonc.2020.599073

Li, T., Mello-Thoms, C., and Brennan, P. C. (2016). Descriptive Epidemiology of Breast Cancer in China: Incidence, Mortality, Survival and Prevalence. *Breast Cancer Res. Treat.* 159, 395–406. doi:10.1007/s10549-016-3947-0

Liu, C., Wang, K., Zhuang, J., Gao, C., Li, H., Liu, L., et al. (2019). The Modulatory Properties of Astragalus Membranaceus Treatment on Triple-Negative Breast Cancer: An Integrated Pharmacological Method. *Front. Pharmacol.* 10, 1171. doi:10.3389/fphar.2019.01171

Lu, X., Zheng, Y., Wen, F., Huang, W., and Shu, P. (2020). Effectiveness and Safety of Oral Chinese Patent Medicines Combined with Chemotherapy for Gastric Cancer: A Bayesian Network Meta-Analysis. *Evid. Based Complement. Alternat Med.* 2020, 8016531. doi:10.1155/2020/8016531

Martinez-Outschoorn, U. E., Peiris-Pagés, M., Pestell, R. G., Sotgia, F., and Lisanti, M. P. (2017). Cancer Metabolism: a Therapeutic Perspective. *Nat. Rev. Clin. Oncol.* 14, 11–31. doi:10.1038/nrclinonc.2016.60

Miller, K. D., Nogueira, L., Mariotto, A. B., Rowland, J. H., Yabroff, K. R., Alfano, C. M., et al. (2019). Cancer Treatment and Survivorship Statistics, 2019. *CA Cancer J. Clin.* 69, 363–385. doi:10.3322/caac.21565

Pavlova, N. N., and Thompson, C. B. (2016). The Emerging Hallmarks of Cancer Metabolism. *Cell Metab* 23, 27–47. doi:10.1016/j.cmet.2015.12.006

Pondé, N. F., Zardavas, D., and Piccart, M. (2019). Progress in Adjuvant Systemic Therapy for Breast Cancer. *Nat. Rev. Clin. Oncol.* 16, 27–44. doi:10.1038/s41571-018-0089-9

Poo, C. L., Dewadas, H. D., Ng, F. L., Foo, C. N., and Lim, Y. M. (2021). Effect of Traditional Chinese Medicine on Musculoskeletal Symptoms in Breast Cancer: A Systematic Review and Meta-Analysis. *J. Pain Symptom Manage.* 62, 159–173. doi:10.1016/j.jpainsymman.2020.11.024

Sha, Q., Lyu, J., Zhao, M., Li, H., Guo, M., and Sun, Q. (2020). Multi-Omics Analysis of Diabetic Nephropathy Reveals Potential New Mechanisms and Drug Targets. *Front. Genet.* 11, 616435. doi:10.3389/fgene.2020.616435

Sung, H., Ferlay, J., Siegel, R. L., Laversanne, M., Soerjomataram, I., Jemal, A., et al. (2021). Global Cancer Statistics 2020: GLOBOCAN Estimates of Incidence and Mortality Worldwide for 36 Cancers in 185 Countries. *CA Cancer J. Clin.* 71, 209–249. doi:10.3322/caac.21660

Tabe, Y., Lorenzi, P. L., and Konopleva, M. (2019). Amino Acid Metabolism in Hematologic Malignancies and the Era of Targeted Therapy. *Blood* 134, 1014–1023. doi:10.1182/blood.2019001034

Tao, J. J., Visvanathan, K., and Wolff, A. C. (2015). Long Term Side Effects of Adjuvant Chemotherapy in Patients with Early Breast Cancer. *Breast* 24 Suppl 2 (Suppl. 2), S149–S153. doi:10.1016/j.breast.2015.07.035

Thévenot, E. A., Roux, A., Xu, Y., Ezan, E., and Junot, C. (2015). Analysis of the Human Adult Urinary Metabolome Variations with Age, Body Mass Index, and Gender by Implementing a Comprehensive Workflow for Univariate and OPLS Statistical Analyses. *J. Proteome Res.* 14, 3322–3335. doi:10.1021/acs.jproteome.5b00354

Untch, M., Konecny, G. E., Paepke, S., and von Minckwitz, G. (2014). Current and Future Role of Neoadjuvant Therapy for Breast Cancer. *Breast* 23, 526–537. doi:10.1016/j.breast.2014.06.004

Vander Heiden, M. G., Cantley, L. C., and Thompson, C. B. (2009). Understanding the Warburg Effect: the Metabolic Requirements of Cell Proliferation. *Science* 324, 1029–1033. doi:10.1126/science.1160809

Wu, J., Liu, Y., Fang, C., Zhao, L., Lin, L., and Lu, L. (2019). Traditional Chinese Medicine Preparation Combined Therapy May Improve Chemotherapy Efficacy: A Systematic Review and Meta-Analysis. *Evid. Based Complement. Alternat Med.* 2019, 5015824. doi:10.1155/2019/5015824

Xiang, Y., Guo, Z., Zhu, P., Chen, J., and Huang, Y. (2019). Traditional Chinese Medicine as a Cancer Treatment: Modern Perspectives of Ancient but Advanced Science. *Cancer Med.* 8, 1958–1975. doi:10.1002/cam4.2108

Yan, Z., Lai, Z., and Lin, J. (2017). Anticancer Properties of Traditional Chinese Medicine. *Comb. Chem. High Throughput Screen.* 20, 423–429. doi:10.2174/1386207320666170116141818

Yang, Y., Ting, W., Xiao, L., Shufei, F., Wangxiao, T., Xiaoying, W., et al. (2017). Immunoregulation of Shenqi Fuzheng Injection Combined with Chemotherapy in Cancer Patients: A Systematic Review and Meta-Analysis. *Evid. Based Complement. Alternat Med.* 2017, 5121538. doi:10.1155/2017/5121538

Yang, Z., Zhang, Q., Yu, L., Zhu, J., Cao, Y., and Gao, X. (2021). The Signaling Pathways and Targets of Traditional Chinese Medicine and Natural Medicine in Triple-Negative Breast Cancer. *J. Ethnopharmacol* 264, 113249. doi:10.1016/j.jep.2020.113249

Zhang, Z., Yi, P., Yang, J., Huang, J., Xu, P., Hu, M., et al. (2020). Integrated Network Pharmacology Analysis and Serum Metabolomics to Reveal the Cognitive Improvement Effect of Bushen Tiansui Formula on Alzheimer's Disease. *J. Ethnopharmacol* 249, 112371. doi:10.1016/j.jep.2019.112371

Zhou, R., Chen, H., Chen, J., Chen, X., Wen, Y., and Xu, L. (2018). Extract from Astragalus Membranaceus Inhibit Breast Cancer Cells Proliferation via PI3K/AKT/mTOR Signaling Pathway. *BMC Complement. Altern. Med.* 18, 83. doi:10.1186/s12906-018-2148-2

Conflict of Interest: The authors declare that the research was conducted in the absence of any commercial or financial relationships that could be construed as a potential conflict of interest.